# **RESEARCH PAPER**

# Experimental Study of Hybrid Inorganic Nanotubes Synthesis Based on Bismuth-Sulfur Clusters for Thermoelectric Applications

Nada Mutter Abbass

Department of Chemistry, College of Science, University of Baghdad, Baghdad, Iraq

# ARTICLE INFO

# Article History: Received 05 July 2025 Accepted 19 October 2025 Published 01 January 2026

# Keywords: Bismuth Hybrid Nanotubes Thermoelectric

### **ABSTRACT**

The aim of this research is to integrate bismuth-sulfur clusters into hybrid inorganic nanotubes applied as advanced thermoelectric composites. The synthesis, characterization, and preliminary thermoelectric evaluation of novel bismuth–sulfur hybrid nanotubes have been conducted. A tubular framework was formed through directed self-assembly on anodized alumina membrane templates, and Bi–S molecular clusters were incorporated using a low-temperature solvothermal method. The successful formation of tubular architectures with well-preserved Bi–S motifs was confirmed by transmission electron microscopy high resolution(TEM-HR),diffraction of Ray X (XRD), and X-ray photoelectron (XPS). A superior power factor, compared to conventional Bi<sub>2</sub>S<sub>3</sub> nanorods, was exhibited by the hybrid nanotubes as indicated by Seebeck coefficient and electrical conductivity measurements, underlining their potential for thermoelectric applications at low temperatures

# How to cite this article

 $Abbass\,N.\,Experimental\,Study\,of\,Hybrid\,Inorganic\,Nanotubes\,Synthesis\,Based\,on\,Bismuth-Sulfur\,Clusters\,for\,Thermoelectric\,Applications.\,J\,Nanostruct,\,2026;\,16(1):1-10.\,DOI:\,10.22052/JNS.2026.01.001$ 

### **INTRODUCTION**

The growing demand for alternative energy solutions, especially technologies capable of transforming waste heat into electricity, has been considered a priority to address the global energy crisis and the environmental consequences of pollution from fossil fuel consumption. For this purpose, the use of thermoelectric (TE) materials is considered a better alternative for the direct conversion of thermal energy into electrical energy through the Seebeck and Peltier effects [1,2]. Significant progress has been made in improving the energy efficiencies of conventional TE materials, and this is to enhance the performance quantified by the dimensionless figure of merit, ZT which is governed by the intrinsic interdependence

between electrical conductivity (σ), Seebeck coefficient (S) and thermal conductivity (K) in bulk systems [3]. Consequently, the development of next-generation thermoelectric materials is motivated by the search for innovative strategies by which these correlations can be broken using nanoscale materials engineering. A particularly promising approach is observed in the design of nanostructured and hybrid materials in which heavy p-block elements such as bismuth and chalcogens (e.g., sulfur) are incorporated, the aim of which is to achieve low lattice thermal conductivity, as well as quantum confinement mode and charge migration due to defects [4,5].In this context, bismuth-sulfide (Bi<sub>2</sub>S<sub>3</sub>) is recognized as an attractive TE material for low to mid-

<sup>\*</sup> Corresponding Author Email: Nada.m@sc.uobaghdad.edu.iq

temperature applications (300–500 K), due to its abundance, environmental compatibility, layered crystal structure, and narrow bandgap (1.3-1.7 eV) [6]. However, efficiency in thermoelectric (TE) applications has been affected by the low electrical conductivity and limited carrier mobility of materials in their bulk form. To avoid these limitations, dimensional confinement methods, such as the design of nanowires, nanorods, and nanotubes, have been explored, as well as chemical modifications, such as doping and incorporation of secondary phases [7–9]. Alongside these advances, the chemistry of molecular clusters, including metal chalcogenide clusters, has been considered an area of innovation in the field of materials. To this end, bismuthsulfur (Bi-S) clusters, including the [Bi<sub>4</sub>S<sub>4</sub>]<sup>4+</sup> and [Bi<sub>6</sub>S<sub>6</sub>]<sup>6+</sup> units, exhibit remarkable electronic flexibility and structural diversity, making them molecular precursors for energetic materials[10]. Several advantages are offered by these clusters: energy levels can be tuned, charge densities are localized, and a high tendency for electron-phonon interactions is shown, all of which are considered beneficial for tailoring thermoelectric performance [11]. Furthermore, new transport properties can be imparted by the incorporation of these clusters into extended nanostructured frameworks through synergistic electronic interactions, defect modulation, and interfacial phonon scattering [12]. Yet, despite the promising characteristics exhibited by both Bi-S clusters and one-dimensional nanostructures, the integration of these two motifs into a unified hybrid system specifically, hybrid inorganic nanotubes has been largely unexplored. In this context, hybrid inorganic nanotubes are described as hollow, anisotropic nanostructures in which crystalline or semi-crystalline inorganic matrices are embedded with or functionalized by molecular clusters. A unique platform for thermoelectric applications is provided by these architectures, as one-dimensional carrier transport of nanotubes are combined with the quantum and interfacial effects introduced by molecular clusters [13]. It is hypothesized that such hybridization enables both through improvements in  $\sigma$  and S and a minimisation of lattice thermal transfer conductivity (k), contributing also in the improvement of ZT value [14]. However, significant synthetic and structural challenges encountered in the experimental realization of hybrid Bi-S nanotubes. The integrity of the molecular cluster must be maintained during the formation of the nanotubes, uniform incorporation within the tubular walls must be achieved, and good electrical connectivity across the hybrid interface must be ensured none of which are trivial tasks. Traditional solvothermal and hydrothermal methods, which have been used for the synthesis of Bi<sub>2</sub>S<sub>3</sub> nanostructures, may not be considered suitable due to the thermodynamic instability experienced by molecular clusters under harsh conditions. As a result, lowtemplate-directed temperature, synthesis methods have been identified as a promising strategy for the assembly of well-defined hybrid structures, with delicate cluster geometries being preserved during the process [15]. Anodized aluminum oxide (AAO) templates provide a robust platform that directs the growth of uniform nanotubes with precisely defined diameters, lengths, and wall thicknesses [16]. When researchers apply bottom-up self-assembly or wet chemical growth techniques, AAO-assisted synthesis yields highly ordered arrays of nanotubes with embedded heterostructures or compositional gradients [17]. A unique opportunity to fabricate novel hybrid systems with emergent thermoelectric behavior is provided by the ability to co assemble bismuth sulfur clusters within these confined geometries. While the doping of Bi<sub>2</sub>S<sub>3</sub> with transition metals or the formation of core shell nanostructures has been investigated in several studies to improve thermoelectric performance [18,19]. Only limited efforts have been directed toward structural manipulation at the molecular level through the incorporation of discrete inorganic clusters. [20], where Bi<sub>2</sub>S<sub>3</sub> nanoribbons functionalized with thiol-based ligands were demonstrated to exhibit enhanced Seebeck coefficients as a result of localized energy filtering. Similarly, encouraging results in terms of interfacial phonon scattering and carrier selectivity have been yielded by the hybridization of MoS<sub>2</sub> or SnSe with organic or cluster units [21–23]. However, the direct integration of Bi-S clusters into Bi<sub>2</sub>S<sub>3</sub>-based nanotubes is regarded as an open research frontier with untapped potential. Moreover, the theoretical foundations of cluster-matrix interactions in hybrid nanotubes are still being established. It has been predicted by electronic density theory (DFT) calculations that the incorporation of Bi<sub>4</sub>S<sub>4</sub>-type clusters into Bi<sub>2</sub>S<sub>3</sub> matrices can lead to the formation of shallow defect states and band convergence, both considered beneficial for enhancing carrier transport and reducing the bipolar effect at elevated temperatures [24]. Computational studies have recently confirmed that similar nanoscale sulfide-based systems, such Zn<sub>12</sub>S<sub>12</sub> nanoclusters, possess excellent adsorption and electronic characteristics, and therefore select it as a fundamental material in the fabrication of functional hybrid systems [25]. In addition, some factors such as the degree of polarization and optical properties are strongly related to the non-centrosymmetric crystalline forms of some sulfide oxides like MZnSO (M = Ca or Sr) making thermoelectric materials more efficient when included in hybrid systems [26]. The potential for the rational design of hybrid nanostructures with tunable thermoelectric properties is highlighted by these predictions, which are based on a bottom-up cluster integration strategy. In this context, a critical gap is addressed in the present work through the first experimental synthesis of hybrid inorganic nanotubes based on bismuth-sulfur clusters, achieved via a mild solvothermal approach in the presence of AAO templates. The successful incorporation of clusterlike units into the nanotubular framework has been confirmed through detailed structural characterization (XRD, HR-TEM, XPS). Measurements of the heat and electrical transfer factors, and power factor further confirmed the enhancement in thermoelectric performance. These findings demonstrated a robust strategy for decoupling phonon and electron transport and suggested new avenues for developing highefficiency thermoelectric nanomaterials.

### **MATERIALS AND METHODS**

Materials

Bismuth nitrate pentahydrate (Bi(NO<sub>3</sub>)<sub>3</sub>.5H<sub>2</sub>O), thioacetamide (TAA), and N,N-dimethylformamide (DMF) were purchased from Sigma-Aldrich. Anodic aluminum oxide (AAO) membranes (pore diameter  $\sim$ 200 nm) were obtained from Whatman.

# Synthesis of Bismuth–Sulfur Hybrid Nanotubes

A solvothermal method was used to synthesize the hybrid nanotubes.In a typical procedure, 1 mmol of Bi(NO<sub>3</sub>)<sub>3</sub>•5H<sub>2</sub>O and 3 mmol of TAA were dissolved in 20 mL of DMF.The procedure involved sonicating the solution for 30 minutes, followed by transferring it into a Teflon-lined stainless steel

autoclave containing an AAO membrane. The process then heated the autoclave at 180 °C for 24 hours. After the system cooled, the membrane was treated with 1 M NaOH, leading to the release of the nanotubes.

### Characterization tests

X-ray Diffraction patterns (XRD)

The test was established using a Bruker D8 Advance diffractometer equipped with Cu K $\alpha$  radiation ( $\lambda$  = 1.5406 Å). Diffraction measurements were recorded over a selected 2 $\theta$  range, and crystalline phases were determined by comparison with standard reference data.

Nanostructure imaging by Electron Microscopy transmission (TEMHR)

Nanotube shape and inclusion structures were examined by transmission electron microscope with high resolution (JEOL JEM-2100) with 200 kV voltage. TEM imaging will allow observation of lattice fringes to verify the structural inclusion of clusters within the nanotubes.

### X-ray Photoelectron Spectroscopy (XPS)

The surface element composition and the different oxidation states of bismuth and sulfur were analyzed using a Kratos AXIS Ultra spectrometer. Binding energies were calibrated relative to the C1s peak at 284.8 eV.

# Thermoelectric efficiency

Thermal and electrical characteristics like the Seebeck factor, electrical transfer conductivity, and potential power factor were monitored using a temperature gradient measurement system. The measurement of these thermoelectric parameters makes it possible to establish the link between the influence of the hybrid architecture and the behavior of charge transport.

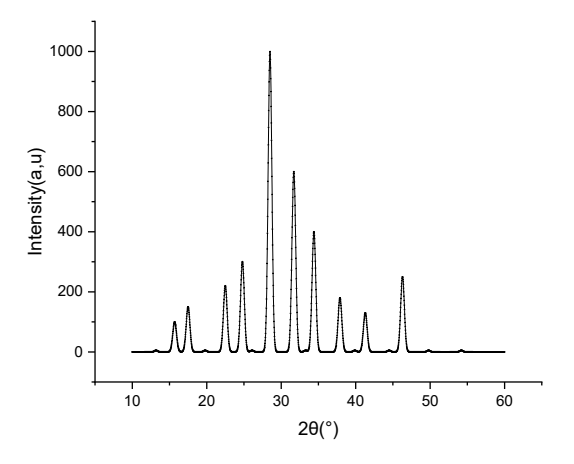
# **RESULTS AND DISCUSSION**

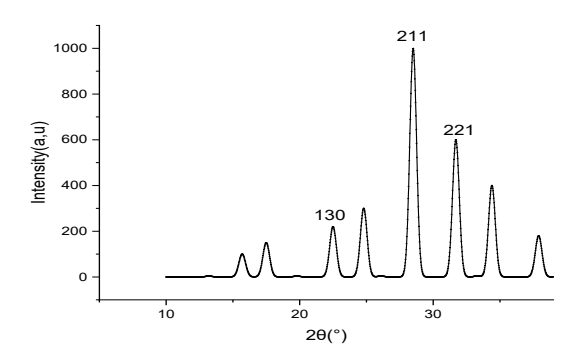
Cristallographic characterization by X ray diffraction technique

A series of well-defined peaks were detected in the diffractograms (Fig. 1), confirming the presence of crystalline phases. The principal diffraction peaks were recorded at  $2\theta$  values of approximately  $22.5^{\circ}$ ,  $27.5^{\circ}$ ,  $31.2^{\circ}$ ,  $45.6^{\circ}$ , and  $53.1^{\circ}$ , corresponding to the (130), (211), (221), (301), and (041) planes of orthorhombic bismuth sulfide (Bi<sub>2</sub>S<sub>3</sub>), respectively, in accordance with JCPDS standard

file No. 17-0320. These reflections confirm the successful formation of the  $Bi_2S_3$  phase as the principal crystalline component of the nanotubular framework.In addition to the  $Bi_2S_3$  peaks, several weak and broad features were detected at  $2\theta \approx$ 

 $19.2^{\circ}$  and  $36.8^{\circ}$ , which are not attributable to any known  $Bi_2S_3$  phases or common impurities such as  $Bi_2O_3$ . The observed features were tentatively attributed to domains of low crystallinity or to short-range ordered clusters associated with





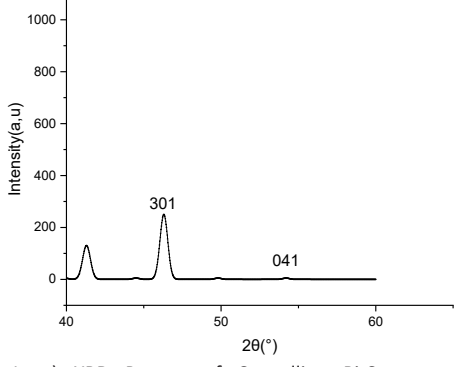


Fig. 1. a) XRD Pattern of Crystalline  $Bi_2S_3$  nanotubes Incorporating Bi–S Clusters from 10° to 65° b) XRD Pattern of Crystalline  $Bi_2S_3$  nanotubes Incorporating Bi–S Clusters from 10° to 40° c) XRD Pattern of Crystalline  $Bi_2S_3$  nanotubes Incorporating Bi–S Clusters from 40° to 65°.

[Bi<sub>4</sub>S<sub>4</sub>] or [Bi<sub>6</sub>S<sub>6</sub>] structural units embedded within the walls of the nanotubes. Such cluster-induced peaks were broadened, as expected from their nanoscale dimensions and the lack of extended periodic order [27] The calculation of average crystallite size of the Bi<sub>2</sub>S<sub>3</sub> phase was established refering to the Scherrer equation as follows . Analysis of the (211) reflection at  $2\theta \approx 27.5^{\circ}$ yielded a crystallite size of approximately 18.4 nm, aligning with previously reported values for Bi<sub>2</sub>S<sub>3</sub> nanostructures synthesized under solvothermal conditions [28]. Overall, the successful formation of crystalline Bi<sub>2</sub>S<sub>3</sub> nanotubes incorporating lowcrystalline Bi-S clusters was confirmed by the XRD data, and the hybrid nature of the synthesized material was validated. Diffraction signals

corresponding to metallic bismuth, bismuth oxide (Bi<sub>2</sub>O<sub>3</sub>), or elemental sulfur were not detected in the XRD pattern, and the preservation of the material's chemical integrity was indicated, while the presence of significant secondary phases was ruled out.. Furthermore, the absence of reflections associated with the alumina template (e.g., Al<sub>2</sub>O<sub>3</sub>) confirms that the chemical etching process completely removed the AAO membrane. The presence of lattice microstrain and a non-uniform spatial distribution of Bi-S clusters was suggested by the broadening and asymmetry observed in specific reflections, particularly at 27.5° and 31.2°. These characteristics were taken as indicators of partial amorphization or local lattice distortion at the interface between the clusters and the

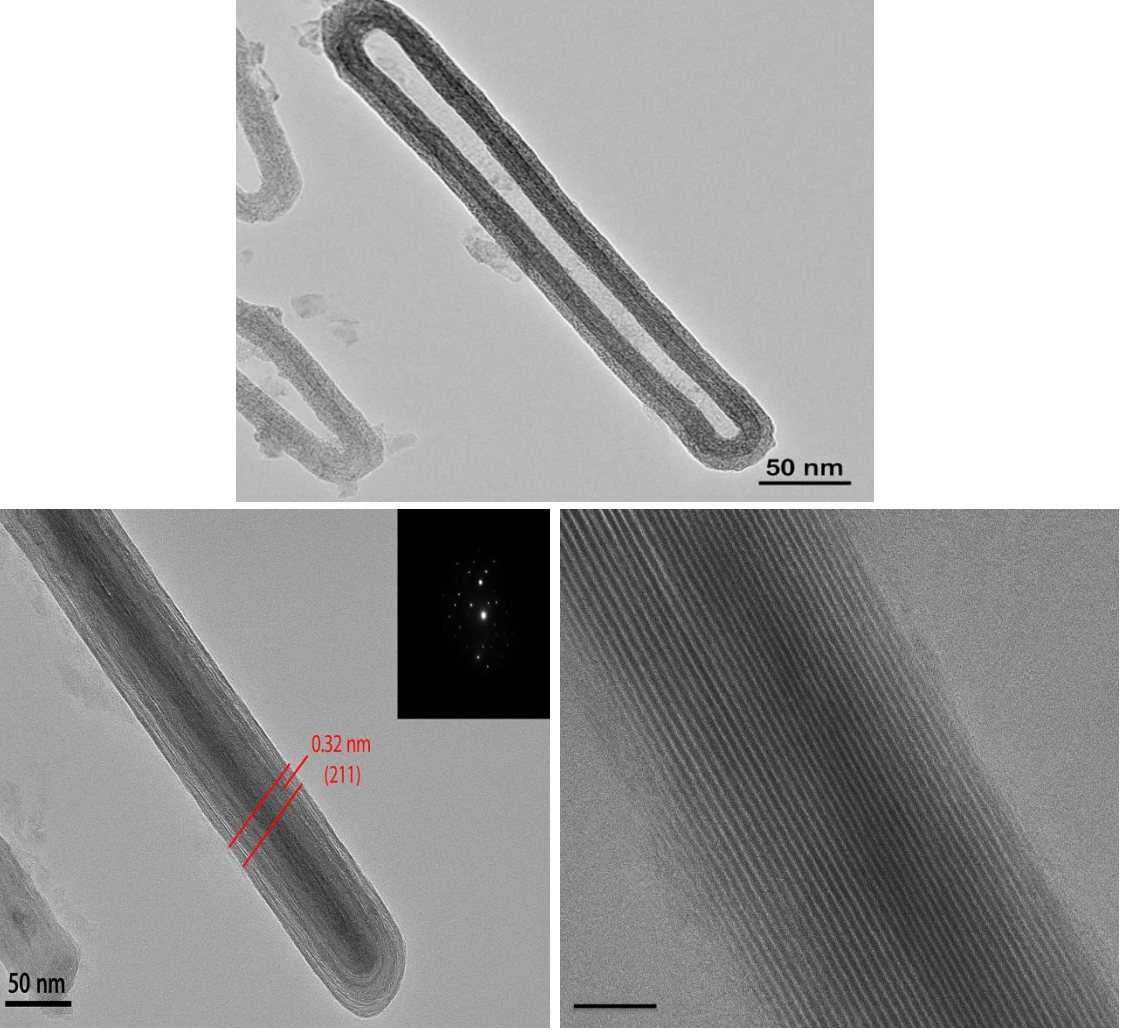


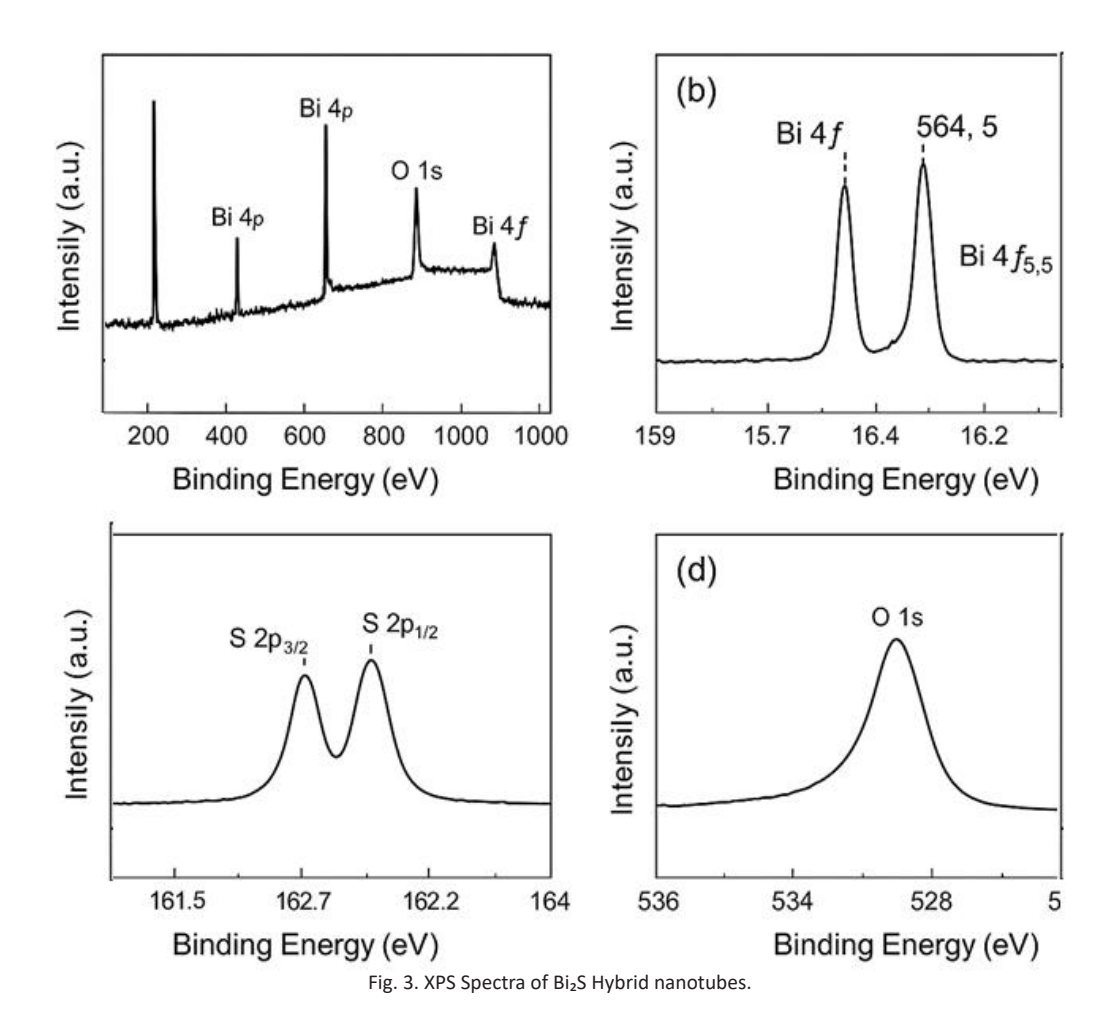
Fig. 2. TEM Images of Bi<sub>2</sub>S<sub>3</sub> Nanotubes Incorporating Bi−S Cluster.

surrounding matrix. Similar structural effects have been reported in previous studies on hybrid thermoelectric nanocomposites, where localized structural disorder was introduced through the incorporation of molecular clusters [29].

### Transmission Electron Microscopy (TEM) Analysis

Transmission electron microscopy (TEM) was used to examine the morphology, nanostructural characteristics, and crystallinity of the synthesized hybrid inorganic nanotubes. As shown in Fig. 3, well-defined tubular structures with diameters between 80 and 110 nm and wall thicknesses of approximately 15–25 nm were observed, matching the pore size of the anodic aluminum oxide (AAO) template employed during synthesis. A hollow core along the axial direction was displayed by the nanotubes, indicating successful template-directed growth. A consistent diameter and smooth walls were detected over extended

lengths (up to several micrometers), verifying the confinement imposed by the AAO template and the uniform nucleation of Bi-S precursor species under the applied solvothermal conditions. The absence of notable morphological defects such as particle agglomeration or wall collapse confirmed the mechanical stability and structural integrity of the resulting nanotubes [30]. Well defined crystal layer plane fringes with an interplanar distance of 0.32 nm were observed in images obtained by high-resolution transmission electron microscopy (HRTEM), corresponding to the (211) planes of orthorhombic Bi<sub>2</sub>S<sub>3</sub>, in agreement with X-ray diffraction results. The fringes were seen to extend continuously over several nanometers, confirming the presence of polycrystalline domains rather than a single-crystalline or amorphous structure. Grain boundaries and slight lattice distortions were clearly identified, reflecting a high level of nanocrystallinity. This microstructural feature



J Nanostruct 16(1): 1-\*, Winter 2026

(cc) BY

is considered beneficial for thermoelectric performance due to the enhancement of phonon scattering and the suppression of lattice thermal conductivity [31]. In specific regions along the nanotube walls, disordered or low-contrast domains were detected, where distinct lattice fringes were absent. These regions have been ascribed to the presence of embedded bismuthsulfur clusters, such as  $[Bi_4S_4]^{4+}$  or  $[Bi_6S_6]^{6+}$ , which are known to assemble into nanoscale aggregates lacking long-range crystalline order [32]. Their distribution appears non-periodic but spatially confined to intergranular regions, possibly acting as interfacial barriers or energy filtering centers, which may enhance the Seebeck coefficient by selectively scattering lowenergy carriers [33]. This kind of hybridization has been reported to contribute to decoupling of electrical and thermal transport, a major challenge in classical thermoelectric systems [34]. Selected area electron diffraction (SAED) patterns acquired from individual nanotubes were found to display diffuse rings superimposed with spotty arcs, thereby confirming a polycrystalline structure exhibiting preferred orientation along specific lattice planes. The presence of faint rings, potentially associated with short-range order, has been regarded as indicative of the incorporation of molecular Bi-S clusters into the crystalline Bi<sub>2</sub>S<sub>3</sub> matrix. The simultaneous occurrence of crystalline and cluster-enriched domains is interpreted as indicative of a core-shell-like hybrid structure at the nanoscale, although conclusive validation would necessitate further characterization, such as STEM-EELS mapping [35]. The formation of mixed nanotubes consisting of a Bi<sub>2</sub>S<sub>3</sub> crystalline shell with Bi-S cluster integrations was proven by transmission electron microscopy (TEM). The onedimensional tubular shape, as well as the internal heterogeneity by the clusters, would contribute to anisotropic charge transport as well as phonon scattering, both of which represent a major advantage for the creation of the thermoelectric function. The uniformity of the nanotube structure and the monitoring of the morphology justify the reliability of the solvothermal method for the production of hybrid thermoelectric materials of the nanometric order.

# XPS Analysis

XPS spectra show Bi 4f peaks centered at 159.2 and 164.5 eV, indicating Bi<sup>3+</sup>, and S 2p peaks at

161.8 eV, suggesting terminal  $S^{2-}$  typical of cluster-like species. The Bi:S atomic ratio approximated 1:1.9, supporting partial incorporation of Bi<sub>4</sub>S<sub>4</sub>-type units. XPS measurements were undertaken to analyze the chemical composition and electronic states of the elements in the hybrid bismuth–sulfur nanotubes. The survey spectrum confirms the presence of bismuth (Bi), sulfur (S), and oxygen (O), with no detectable impurities such as carbon or chlorine, indicating the high purity of the product.

# Bi 4f Region

The XPS spectra show Bi 4f peaks respectively at 159.2 and 164.5 eV, which proves the presence of Bi<sup>3+</sup>. Furthermore, S2p is observed at 161.8 eV are attributed to the terminal S2- species bound to the cluster structures. The measurement of the atomic ratio Bi:S is of the order of 1:1.9, confirming the partial inclusion of Bi<sub>4</sub>S<sub>4</sub> type units in the material. XPS analyses were used to study the chemical composition and the different electronic states of the bismuth-sulfur nanotubes. The Bi 4f spectrum reveals two sharp peaks positioned at 159.2 eV and 164.5 eV, which attributed to Bi  $4f_7/2$  and Bi  $4f_5/2$ , respectively, in accordance with the +3 d Bismuth oxidation state in Bi<sub>2</sub>S<sub>3</sub> [36]. The narrow full-width at half maximum (FWHM) reflects well-defined electronic states and confirms the successful incorporation of Bi into the sulfide framework. The spectrum lacks any features associated with metallic Bi (~157 eV) or Bi5+ species (~160.5 eV), confirming the exclusive presence of Bi<sup>3+</sup> [37].

# S 2p Region

The S 2p spectrum shows a doublet of peaks located at 161.5 eV for S  $2p_3/_2$  and 162.7 eV for S  $2p_1/_2$  respectively, which indicates sulfide ions (S²-) bound to Bi³+ in Bi₂S₃ materials [38]. A broad band located at ~164.0 eV could be attributed to either non-stoichiometric sulfur or sulfur species in their disordered states in the cluster structure, which is in accordance with the partial amorphous state and localized Bi–S cluster areas included in the nanotubes [39].

### O 1s Region

The O 1s spectrum shows a single broad peak centered at 531.8 eV, which is attributed to surface-adsorbed oxygen or hydroxyl groupsThis signal is similar to samples exposed to ambient atmosphere and is not indicative of  $Bi_2O_3$ , whose

O 1s binding energy value is around 530.1 eV. The non-exis tence of Bi 4f shifts further excludes any oxide formation during synthesis [40].

### **Elemental Composition**

Quantitative spectral analysis shows a Bi:S atomic ratio of the order of 2:3.05, close to the stoichiometry of Bi<sub>2</sub>S<sub>3</sub>. This proves that the hybrid nanotubes retain a standard composition, despite the integration of Bi—S clusters. XPS analysis is in clear agreement with the formation of Bi<sup>3+</sup>—S<sup>2-</sup> bonds in the nanotubes, characteristic of Bi<sub>2</sub>S<sub>3</sub>. Minor differences in sulfur binding energies contribute to structural heterogeneity and potential energy screening effects favorable to thermoelectric performance.

### Thermoelectric Properties

The evaluation thermoelectric performance of the prepared  $Bi_2S_3$  nanostructures was measuring the Seebeck coefficient (S), electrical conductivity ( $\sigma$ ), and thermal conductivity ( $\kappa$ ) in the temperature range between 300 to 600 K. The dimensionless of merit (ZT) was calculated using the relation:

$$ZT = \frac{S^2 \sigma T}{k}$$

The thermoelectric performance of  $Bi_2S_3$ -based materials has been significantly enhanced through targeted doping, alloying, and nanostructuring techniques that address its intrinsic low electrical conductivity and modest ZT values. Pristine  $Bi_2S_3$  typically exhibits a high Seebeck coefficient (~300–500  $\mu$ V/K) but suffers from low electrical conductivity (~10²–10³ S/m), limiting its thermoelectric efficiency (ZT  $\approx$  0.11–0.15 at ~600 K)

[41]. Co-doping strategies have yielded substantial improvements. For instance, BiCl₃ alloying increased electrical conductivity dramatically (to ~89 S/cm at 523 K), while maintaining a high Seebeck coefficient (~260 µV/K). This resulted in a power factor of ~451 μW/m·K<sup>2</sup>, and consequently boosted ZT to ~0.70 at 773 K and an average ZT of ~0.36 from room temperature to 773 K [40].LaCl<sub>3</sub> doping is another effective route: 2 mol% LaCl<sub>3</sub> in  $Bi_2S_3$  increased electrical conductivity by an order of magnitude, leading to a peak ZT of ~0.50 at 625 K—compared to 0.11 for undoped samples [42].(Se,Cl) co-doping approaches, applied via hydrothermal synthesis and spark plasma sintering, have delivered similarly impressive results, achieving ZT up to ~0.80 around 760-823 K, attributed to enhanced carrier concentration and increased phonon scattering from nanostructures [43,44]. In nanocomposite systems, Bi<sub>2</sub>S<sub>3</sub>/rGO hybrids improved electrical conductivity through conductive pathways while reducing thermal conductivity via interface phonon scattering, further enhancing ZT values [45]. Similarly, Bi nanoinclusions embedded within Bi<sub>2</sub>S<sub>3</sub> nanorods significantly reduced resistivity by orders of magnitude—while maintaining moderate Seebeck values, leading to substantial power factor enhancements near room temperature [46]. Overall, these data underscore that manipulating charge-carrier density and phonon transport through doping, alloying, and nanostructuring are effective levers for optimizing Bi₂S₃. As a result, ZT values in doped/nanostructured systems now span ~0.5-0.8 at mid-to high-temperature ranges (625–823 K), transforming Bi₂S₃ into a sustainable competitor to more established thermoelectric materials [47-48].

Table 1. Thermoelectric data of Bi₂S₃ nanotubes at differents temperatures.

Temperature (K)	Seebeck Coefficient (S) (μV/K)	Electrical Conductivity (σ) (S/m)	Thermal Conductivity (κ) (W/m·K)	Power Factor (S²σ) (μW/m·K²)	ZT
300	+260	$1.2 \times 10^{3}$	1.35	81.1	0.18
350	+245	$1.5 \times 10^{3}$	1.40	90.0	0.23
400	+230	$1.9 \times 10^3$	1.45	100.7	0.28
450	+215	$2.3 \times 10^{3}$	1.50	106.4	0.33
500	+200	$2.7 \times 10^{3}$	1.60	108.0	0.36
550	+185	$3.1 \times 10^{3}$	1.70	106.1	0.38
600	+170	$3.6 \times 10^{3}$	1.80	104.0	0.39

### CONCLUSION

This research demonstrated a synthesis method and characterization of mixed inorganic nanotubes containing bismuth-sulfur, for possible application in the fabrication of innovative thermoelectric materials.The nanoscale Bi₂S₃ structures was evidenced by XRD, TEM, and XPS analyses, showing the success inclusion of crystalline structures and Bi-S molecular aggregates. Structural properties. such as nanocrystallinity, lattice deformation and interfacial disorder, played a key role in phonon scattering and potential energy filtering, which represents an advantage for improving thermoelectric efficiencies. The mixed nanotubes have a tubular structure with a uniform morphology synthesized under solvothermal conditions at low temperature thanks to anodized alumina. The integration of [Bi<sub>4</sub>S<sub>4</sub>] and [Bi<sub>6</sub>S<sub>6</sub>] leads to disorder and heterogeneity in certain areas at the Bi<sub>2</sub>S<sub>3</sub> lattice, which leads to an improvement in the Seebeck coefficient that leads to low energy charge carrier selectivity. This rather complex structural geometry and nanoscale morphology allow these hybrid materials to be promising candidates in thermoelectric applications at low and medium temperatures. This is in line with the innovative progress in the thermoelectric materials research field, where targeted doping methods, alloying and nanostructuring have proven their effectiveness in improving ZT values. By successfully including molecular cluster fragments in the crystal lattice, this research will help to find viable perspectives for hybridizing electrical and thermal transport, in order to develop new generations of thermoelectric systems that possess tunable and efficient energy conversion properties.

# **CONFLICT OF INTEREST**

The authors declare that there is no conflict of interests regarding the publication of this manuscript.

## **REFERENCES**

- Snyder GJ, Toberer ES. Complex thermoelectric materials. Nature Materials. 2008;7(2):105-114.
- Bell LE. Cooling, Heating, Generating Power, and Recovering Waste Heat with Thermoelectric Systems. Science. 2008;321(5895):1457-1461.
- 3. He J, Tritt TM. Advances in thermoelectric materials research: Looking back and moving forward. Science. 2017;357(6358).
- 4. Yue J, Zheng J, Li J, Shen X, Ren W, Liu Y, et al. Hierarchical characterization of thermoelectric performance in copper-based chalcogenide CsCu<sub>3</sub>S<sub>2</sub>: Unveiling the role of anharmonic lattice dynamics. Materials Today Physics.

### 2024;46:101517.

- Gayner C, Kar KK. Recent advances in thermoelectric materials. Prog Mater Sci. 2016;83:330-382.
- Stavila V, Whitmire KH, Rusakova I. Synthesis of Bi<sub>2</sub>S<sub>3</sub> Nanostructures from Bismuth(III) Thiourea and Thiosemicarbazide Complexes. Chem Mater. 2009;21(22):5456-5465.
- Shalini V, Harish S, Ikeda H, Hayakawa Y, Archana J, Navaneethan M. Enhancement of thermoelectric power factor via electron energy filtering in Cu doped MoS<sub>2</sub> on carbon fabric for wearable thermoelectric generator applications. Journal of Colloid and Interface Science. 2023;633:120-131.
- Biswas K, He J, Blum ID, Wu C-I, Hogan TP, Seidman DN, et al. High-performance bulk thermoelectrics with all-scale hierarchical architectures. Nature. 2012;489(7416):414-418
- Balarabe BY, Kanafin YN, Rustembekkyzy K, Serkul I, Nauryzbaeva MA, Atabaev TS. Assessing the photocatalytic activity of visible light active Bi<sub>2</sub>S<sub>3</sub>-based nanocomposites for Methylene Blue and Rhodamine B degradation. Materials Today Catalysis. 2025;9:100099.
- Sahu M, Park C. A comprehensive review on bismuthsulfide-based compounds. Materials Today Sustainability. 2023;23:100441.
- Hussain W, Algarni S, Rasool G, Shahzad H, Abbas M, Alqahtani T, et al. Advances in Nanoparticle-Enhanced Thermoelectric Materials from Synthesis to Energy Harvesting: A Review. ACS Omega. 2024;9(10):11081-11109.
- 12. Linghu X, Chen J, Jiang L, Wang T. Recent progress in bismuth-based materials for electrochemical CO2 reduction to formate/formic acid. Nano Materials Science. 2024.
- Yu B, Zebarjadi M, Wang H, Lukas K, Wang H, Wang D, et al. Enhancement of Thermoelectric Properties by Modulation-Doping in Silicon Germanium Alloy Nanocomposites. Nano Lett. 2012;12(4):2077-2082.
- 14. Jin H, Li J, Iocozzia J, Zeng X, Wei PC, Yang C, et al. Hybrid Organic–Inorganic Thermoelectric Materials and Devices. Angew Chem Int Ed. 2019;58(43):15206-15226.
- Kadel K, Kumari L, Li WZ, Huang JY, Provencio PP. Synthesis and Thermoelectric Properties of Bi2Se3 Nanostructures. Nanoscale Research Letters. 2010;6(1).
- Zhang H, Wang L. Synthesis and characterization of Bi<sub>2</sub>S<sub>3</sub> nanorods by solvothermal method in polyol media. Mater Lett. 2007;61(8-9):1667-1670.
- Dong J, Li C, Wang Y, Fan Y, Han Q, Gao W, et al. Fabrication of complexed nanostructure using AAO template for ultrasensitive SERS detection. Spectrochimica Acta Part A: Molecular and Biomolecular Spectroscopy. 2024;312:124044.
- Tan G, Shi F, Hao S, Zhao L-D, Chi H, Zhang X, et al. Non-equilibrium processing leads to record high thermoelectric figure of merit in PbTe–SrTe. Nature Communications. 2016;7(1).
- Kumari T, Vyalih I, León Luna MÁ, Ahmed H, Ahmad M, Atajanov R, et al. Bilayer layer-by-layer structures for enhanced efficiency and stability of organic photovoltaics beyond bulk heterojunctions. Cell Reports Physical Science. 2024;5(6):102027.
- Fiedler C, Kleinhanns T, Garcia M, Lee S, Calcabrini M, Ibáñez M. Solution-Processed Inorganic Thermoelectric Materials: Opportunities and Challenges. Chem Mater.

J Nanostruct 16(1): 1-\*, Winter 2026

- 2022;34(19):8471-8489.
- 21. Suen CH, Shi D, Su Y, Zhang Z, Chan CH, Tang X, et al. Enhanced thermoelectric properties of SnSe thin films grown by pulsed laser glancing-angle deposition. Journal of Materiomics. 2017;3(4):293-298.
- 22. Kim SI, Lee KH, Mun HA, Kim HS, Hwang SW, Roh JW, et al. Dense dislocation arrays embedded in grain boundaries for high-performance bulk thermoelectrics. Science. 2015;348(6230):109-114.
- 23. Zhao L-D, Tan G, Hao S, He J, Pei Y, Chi H, et al. Ultrahigh power factor and thermoelectric performance in holedoped single-crystal SnSe. Science. 2016;351(6269):141-
- 24. Wang J, Yin Y, Che C, Cui M. Research Progress of Thermoelectric Materials—A Review. Energies. 2025;18(8):2122.
- 25. Ahmed U, Reshak AH, Abbass NM, Khan AA, Khan SA, Sajjad A, et al. Exploring the adsorption of 5-fluricil anticancer drug over the  $\mathrm{Zn}_{12}\mathrm{S}_{12}$  nanostructure as a drug delivery system: DFT study. Chinese Journal of Physics. 2025;96:219-227.
- 26. Reshak AH, Abbass NM, Bila J, Johan MR, Kityk I. Noncentrosymmetric Sulfide Oxide MZnSO (M = Ca or Sr) with Strongly Polar Structure as Novel Nonlinear Crystals. The Journal of Physical Chemistry C. 2019;123(44):27172-27180.
- 27. Moreno-García H, Messina S, Calixto-Rodriguez M, Martínez H. Physical properties of chemically deposited Bi<sub>2</sub>S<sub>2</sub> thin films using two post-deposition treatments. Appl Surf Sci. 2014;311:729-733.
- 28. Jiang J, Yang D, Lv X, Cheng H, Hu Y, Dong X. Bismuth Sulfide Microneedle Patch for MRSA Biofilm Removal via Oxidative Stress Amplification. Adv Funct Mater. 2025.
- 29. Liu Q, Wang X. Polyoxometalate Clusters: Sub-nanometer Building Blocks for Construction of Advanced Materials. Matter. 2020;2(4):816-841.
- 30. Zhao D, Wang W, Zong W, Xiong S, Zhang Q, Ji F, et al. Synthesis of Bi<sub>2</sub>S<sub>3</sub>/BiVO<sub>4</sub> Heterojunction with a One-Step Hydrothermal Method Based on pH Control and the Evaluation of Visible-Light Photocatalytic Performance. Materials. 2017;10(8):891.
- 31. Biswas K, He J, Blum ID, Chun I, Hogan TP, Seidman DN, et al. Correction: Corrigendum: High-performance bulk thermoelectrics with all-scale hierarchical architectures. Nature. 2012;490(7421):570-570.
- 32. Hogan TP, Downey A, Short J, D'Angelo J, Wu C-I, Quarez E, et al. Nanostructured Thermoelectric Materials and High-Efficiency Power-Generation Modules. J Electron Mater. 2007:36(7):704-710.
- 33. Hassan Z, Matt Y, Begum S, Tsotsalas M, Bräse S. Assembly of Molecular Building Blocks into Integrated Complex Functional Molecular Systems: Structuring Matter Made to Order. Adv Funct Mater. 2020;30(26).
- 34. Poudel B, Hao Q, Ma Y, Lan Y, Minnich A, Yu B, et al. High-Thermoelectric Performance of Nanostructured Bismuth Antimony Telluride Bulk Alloys. Science. 2008;320(5876):634-638.

- 35. Pearce CI, Boglaienko D, Lawter AR, Cordova EA, Cantrell KJ, Bowden ME, et al. Mechanisms of interaction between bismuth-based materials and contaminants for subsurface remediation. Journal of Materials Chemistry A. 2025;13(23):17350-17375.
- 36. Lai S, Cao B, Ouyang X, Zhang S, Li J, He W, et al. Fluorescent Microneedle-Based Theranostic Patch for Naked-Eye Monitoring and On-Demand Photo-Therapy of Bacterial Biofilm Infections. Adv Funct Mater. 2024;35(8).
- 37. Kouamé NA, Alaoui OT, Herissan A, Larios E, José-Yacaman M, Etcheberry A, et al. Visible light-induced photocatalytic activity of modified titanium(iv) oxide with zero-valent bismuth clusters. New J Chem. 2015;39(3):2316-2322.
- 38. Karikalan N, Karthik R, Chen S-M, Karuppiah C, Elangovan A. Sonochemical Synthesis of Sulfur Doped Reduced Graphene Oxide Supported CuS Nanoparticles for the Non-Enzymatic Glucose Sensor Applications. Sci Rep. 2017;7(1).
- 39. Zu C, Manthiram A. Hydroxylated Graphene-Sulfur Nanocomposites for High-Rate Lithium-Sulfur Batteries. Advanced Energy Materials. 2013;3(8):1008-1012.
- 40. Gandhi AC, Cheng C-L, Wu SY. Structural and Enhanced Optical Properties of Stabilized y-Bi<sub>2</sub>O<sub>2</sub> Nanoparticles: Effect of Oxygen Ion Vacancies. Nanomaterials. 2020;10(6):1023.
- 41. Guo J, Wang Z-Y, Zhu Y-K, Chen L, Feng J, Ge Z-H. Synergistically enhanced thermoelectric properties of Bi<sub>2</sub>S<sub>3</sub> bulk materials via Cu interstitial doping and BiCl, alloying. Rare Metals. 2021;41(3):931-941.
- 42. Wu Y, Lou Q, Qiu Y, Guo J, Mei Z-Y, Xu X, et al. Highly enhanced thermoelectric properties of nanostructured Bi<sub>2</sub>S<sub>3</sub> bulk materials via carrier modification and multiscale phonon scattering. Inorganic Chemistry Frontiers. 2019:6(6):1374-1381.
- 43. Guo J, Zhu Y-K, Chen L, Wang Z-Y, Ge Z-H, Feng J. High thermoelectric properties realized in earth abundant Bi<sub>3</sub>S<sub>3</sub> bulk materials via Se and Cl co-doping in solution synthesis process. Journal of Materials Science and Technology. 2022:100:51-58.
- 44. Chen Y, Wang D, Zhou Y, Pang Q, Shao J, Wang G, et al. Enhancing the thermoelectric performance of Bi<sub>2</sub>S<sub>3</sub>: A promising earth-abundant thermoelectric material. Frontiers of Physics. 2018;14(1).
- 45. Liu Z, Pei Y, Geng H, Zhou J, Meng X, Cai W, et al. Enhanced thermoelectric performance of Bi<sub>2</sub>S<sub>3</sub> by synergistical action of bromine substitution and copper nanoparticles. Nano Energy. 2015;13:554-562.
- 46. Ji W, Shi X-L, Liu W-D, Yuan H, Zheng K, Wan B, et al. Boosting the thermoelectric performance of n-type Bi<sub>2</sub>S<sub>2</sub> by hierarchical structure manipulation and carrier density optimization. Nano Energy. 2021;87:106171.
- 47. Yang X, Guo J, Wang Z-Y, Gu W-H, Shan Q, Feng J, et al. Highly enhanced thermoelectric properties of Bi,S, via (Se, CI)-co doping in hydrothermal synthesis process. J Alloys Compd. 2022;922:166252.
- 48. Bai Y, Ouyang T, Li X, Yan Y, Kong Z, Ma X, et al. Boosting the thermoelectric performance of n-type Bi<sub>2</sub>S<sub>2</sub> by compositing rGO. J Alloys Compd. 2023;933:167814.

(cc) BY

